# Segmentation topologique des surfaces discretes

Grégoire Malandain, Gilles Bertrand, Nicholas Ayache

UNITÉ DE RECHERCHE
INRIA-ROCQUENCOURT

Institut National
de Recherche
en Informatique
et en Automatique

Domaine de Voluceau
Rocquencourt
B.P. 105
78153 Le Chesnay Cedex
France
Tél.:(1) 39 63 55 11

Rapports de Recherche

N° 1357

*Programme 6*
*Robotique, Image et Vision*

# SEGMENTATION TOPOLOGIQUE DES SURFACES DISCRÈTES

**Grégoire MALANDAIN, Gilles BERTRAND**
**Nicholas AYACHE**

**Décembre 1990**

*RR-1357*

*Programme 4*

*Robotique, Image et Vision*

# Segmentation Topologique des Surfaces Discrètes

Grégoire MALANDAIN

Gilles BERTRAND

Nicholas AYACHE

Novembre 1990

# Segmentation Topologique des Surfaces Discrètes

Grégoire MALANDAIN
INRIA - Domaine de Voluceau - B.P. 105
78153 LE CHESNAY CEDEX - FRANCE

Gilles BERTRAND
ESIEE - Labo IAAI
Cité Descartes
2, Boulevard Blaise Pascal
93162 NOISY-LE-GRAND CEDEX - FRANCE

Nicholas AYACHE
INRIA - Domaine de Voluceau - B.P. 105
78153 LE CHESNAY CEDEX - FRANCE

# Topological Segmentation of Discrete Surfaces


**Abstract**

We propose in this paper a new approach to segment a discrete 3D object into a structure of characteristic topological primitives with attached qualitative features. This structure can be seen itself as a *qualitative* description of the object, because

- it is intrinsic to the 3D object, which means it is stable to rigid transformations (rotations and translations).
- it is locally defined, and therefore stable to partial occlusions and local modifications of the object structure.
- it is robust to noise and small deformations, as confirmed by our experimental results.

Our approach concentrates on topological properties of discrete surfaces. These surfaces may correspond to the *external* surface of the objects extracted by a 3D edge detector, or to the *skeleton* surface obtained by a new thinning algorithm. Our labeling algorithm is based on very local computations, allowing massively parallel computations and real time computations.

We present a realistic experiment to characterize and locate spatially a complex 3D medical object using the proposed segmentation of its skeleton.


# Segmentation Topologique des Surfaces Discrètes


**Résumé :**

Nous proposons ici une nouvelle approche de segmentation d'objets discrets 3D dans une structure de primitives topologiques caracteéristiques. Cette structure peut être considérée comme une description de l'objet, puisque

- elle est intrinsèque à l'objet 3D, ce qui signifie qu'elle est stable par rapport aux transformations rigides (rotations et translations).
- elle est définie localement donc stable par rapport aux occlusions partielles et aux petites modifications de la structure de l'objet.
- elle est robuste au bruit et aux petites déformations, comme le prouvent nos résultats expérimentaux.

Notre approche se fonde sur les propriétés topologiques des surfaces discrètes. Ces surfaces peuvent être la surface *extérieure* d'objets 3D extraite par un détecteur de contours 3D, ou le squelette obtenu par un algorithme d'amincissement. Notre algorithme de caractérisation topologique ne nécessite que des opérations très locales, ce qui permet une implémentation parallèle et donc des résultats en temps réel.

Nous présentons enfin un exemple réel de caractérisation et de localisation d'un objet médical 3D complexe en utilisant notre segmentation de son squelette.

**Acknowledgements** This work was partially supported by Digital Equipment Corporation and European AIM (Advanced Informatics in Medicine) Project Murim. The authors want to thank Olivier Monga who initialized this research and Pr. J.L. Coatrieux who provided us with the medical images.

# 1 Introduction

Three-dimensional (3-D) images may come from several fields, the most popular one being the medical field, where images are produced by X-ray Computed Tomography (CT), Magnetic Resonance Imaging (MRI), Positon Emitting Tomography (PET), and more recently by Ultrasound Echography.

Automating the *interpretation* of these images is an awkward but important task for many applications where extremely accurate quantitative results are required or/and a large volume of data must be processed. A large class of interpretation tasks involves a *matching* stage, an accurate geometric registration between two 3D images, or between a 3D image and a 3D geometric and semantic model [ABC+90].

Prior to matching, a preliminary *segmentation* stage is necessary to reduce the original image into a more compact highly structured representation useful for interpretation [ABB+89]. We propose in this paper a new segmentation process which transforms a discrete 3D object into a structure of characteristic topological primitives with attached qualitative features. This structure can be seen itself as a *qualitative* description of the object, because

- it is intrinsic to the 3D object, which means it is stable to rigid transformations (rotations and translations).
- it is locally defined, and therefore stable to partial occlusions and local modifications of the object structure.
- it is robust to noise and small deformations, as confirmed by our experimental results.

The idea of characterizing 3D shapes with qualitative primitives was introduced by [San89] who studied differential singularities of 3D object surfaces. Our approach is complementary and original because we concentrate on different topological properties of discrete surfaces instead of geometrical properties. Finally, the core of our approach is based on very local computations, allowing massively parallel computations and real time computations.

This paper is organized as follows : first we recall previous work done on digital topology. Second, we describe our approach which is twofolds, a) local labelling of object points using

a classification tree with two local measures, and b) global extraction of simple surfaces (or surfaces patches), using neighborhood properties. Third, we propose a new thinning algorithm using our classification. Fourth, we present a new distance transformation algorithm, which can compute distance on simple surfaces. Fifth, we describe two applications of this work, one using our thinning algorithm and the other using our classification for the segmentation and the spatial localization of the skeleton of a complex 3D medical object. We conclude this paper by a study of the advantages of this approach and some short and medium term future research topics.

# 2 Basic definitions

We present some basic definitions of 3D digital topology (see [Ros80, KR89, NA85, TYYF82]).

A 3D digital image $\Sigma$ is a subset of $Z^3$. We consider only cubic lattices so that, for each point $x = (i, j, k)$, two types of neighbor may be defined:

**6-neighbors** : $N_6^*(x) = \{y = (i', j', k'), \mid i - i' \mid + \mid j - j' \mid + \mid k - k' \mid = 1\}$

**26-neighbors** : $N_{26}^*(x) = \{y = (i', j', k'), \max(\mid i - i' \mid, \mid j - j' \mid, \mid k - k' \mid) = 1\}$

We note $N_6(x) = N_6^*(x) \cup \{x\}$, $N_{26}(x) = N_{26}^*(x) \cup \{x\}$.

Two subsets $X \subset \Sigma$ and $Y \subset \Sigma$ are said to be 6-adjacent (26-adjacent) if there exist $x \in X$ and $y \in Y$, $x$ and $y$ being 6-neighbors (26-neighbors).

A 6-path (26-path) is a sequence $\rho_0, \rho_1, \ldots \rho_i, \ldots \rho_n$ of points such that $\rho_i$ is 6-adjacent (26-adjacent) to $\rho_{i-1}$, for $1 \leq i \leq n$. An object $X \subset \Sigma$ is 6-connected (26-connected) if a 6-path (26-path) lying in $X$ can be found between each pair of points of $X$.

A 6 (26)-connected component of $X$ is a set $Y \subset X$ which is 6-connected (26-connected) and which is maximal for this property.

As in the 2D-case opposite types of connectedness should be used for $X$ and $\overline{X}$, the complement of $X$.

Hence any further definition has to be viewed as a double definition: a "6-definition" and a "26-definition".

The notion of hole is not simple to define (see [PR71, Mor80]). For example a torus has one hole.

The genus of $X$, $G(X)$ is the number of $X$'s connected components plus the number of its cavities minus the number of its holes.

We have the following relations [Mor80]:

$$G_{26}(\overline{X}) - G_6(X) = 1, \quad G_6(\overline{X}) - G_{26}(X) = 1$$

In [PR71] a method for obtaining the genus of a 3D-object by local pattern matching in the 6-connectedness case is given. In [Mor80] the method for the 26-connectedness case is proposed.

A point $x \in X$ is call simple if its removal does not change the topology of the image.

In [Mor81] a characterization of simple points is proposed. A point $x$ is simple if :

$$NC[X \cap N_{26}(x)] = NC[X \cap N_{26}^{*}(X)] \quad (1)$$

$$NC[(\overline{X} \cap N_{26}^{*}(x)) \cup \{x\}] = NC[\overline{X} \cap N_{26}^{*}(x)] \quad (2)$$

$$NH[X \cap N_{26}(x)] = NH[X \cap N_{26}^{*}(x)] \quad (3)$$

$$NH[(\overline{X} \cap N_{26}^{*}(x)) \cup \{x\}] = NH[\overline{X} \cap N_{26}^{*}(x)] \quad (4)$$

where $NC(A)$ stands for the number of connected components of $A$ and $NH(A)$ denotes the number of holes in $A$. $NH(A)$ may be computed with the genus.

# 3 Connected components numbers

In the continuous space $\Re^3$, we propose a simple way to characterize the points of an object $X$ with local topological properties, which is to examine an arbitrary small neighborhood $V(x)$ of $x \in X$ and to count the number of connected components in $V(x)$ and in $V(x) \setminus \{x\}$. Four connected components numbers may be used:

- $C = NC[X \cap V(x)]$
- $C^{*} = NC[(X \cap V(x)) \setminus \{x\}]$
- $\overline{C} = NC[\overline{X} \cap V(x)]$
- $\overline{C}^{*} = NC[(\overline{X} \cap V(x)) \cup \{x\}]$

For example, if $x$ belongs to a simple surface $X$, there exists $V(x)$ such that $C = 1$, $C^{*} = 1$, $\overline{C} = 2$, $\overline{C}^{*} = 1$. In a complex surface $X$, the curves which are the intersection of several simple surfaces may be characterized by $C = 1$, $C^{*} = 1$, $\overline{C} \geq 3$, $\overline{C}^{*} = 1$. A simple closed curve $X$ is such that there exists $V(x)$ and $C = 1$, $C^{*} = 2$, $\overline{C} = 1$, $\overline{C}^{*} = 1$.

# 4 A new topological classification

We propose to use such connected components numbers to get some information about the local characteristics of points in a 3D digital image.

In the following we assume that 26-connectedness is used for $X$, while 6-connectedness is used for $\overline{X}$. Instead of considering arbitrary small neighborhoods $V(x)$ we use a fixed neighborhood $N_{26}(x)$. For that reason, if we want to get the digital equivalents of the four numbers, we have to consider in the definition of the numbers the components adjacent to $x$ rather that the components being in the neighborhood. Hence, we can define the discrete connected components numbers:

- $C$ = number of 26-components of $X \cap N_{26}(x)$ 26-adjacent to $x$
- $C^*$ = number of 26-components of $[X \cap N_{26}(x)] \setminus \{x\}$ 26-adjacent to $x$
- $\overline{C}$ = number of 6-components of $[\overline{X} \cap N_{26}(x)]$ 6-adjacent to $x$
- $\overline{C}^*$ = number of 6-components of $[\overline{X} \cap N_{26}(x)] \cup \{x\}$ 6-adjacent to $x$

Note that we use 26-adjacency for $X$ and 6-adjacency between $X$ and $\overline{X}$.
We see that, if $x$ belongs to $X$:

1. $C$ is always equal to 1 since all points of $X \cap N_{26}(x)$ are 26-connected to $x$
2. $C^*$ is equal to the number of components of $[X \cap N_{26}(x)] \setminus \{x\}$ for the same reason: $C^* = NC[(X \cap N_{26}(x)) \setminus \{x\}] = NC[X \cap N_{26}^*(x)]$
3. $\overline{C}^*$ is always equal to 1 since all 6-components involved in that number are linked by $x$.

It follows that only two numbers are significant: $C^*$ and $\overline{C}$. We now give a classification of points belonging to $X$ according to the values of $C^*$ and $\overline{C}$:

**Type A** - interior point: $\overline{C} = 0$

**Type B** - isolated point: $\overline{C} = 1,\ C^* = 0$

**Type C** - edge point: $\overline{C} = 1,\ C^* = 1$

**Type D** - curve point: $\overline{C} = 1,\ C^* = 2$

**Type E** - curves junction: $\overline{C} = 1,\ C^* > 2$

**Type F** - surface point: $\overline{C} = 2,\ C^* = 1$

**Type G** - surface - curve junction: $\overline{C} = 2,\ C^* \geq 2$

**Type H** - surfaces junction: $\overline{C} > 2,\ C^* = 1$

**Type I** - surfaces - curve junction: $\bar{C}' \cdot 2$, $C'' \geq 2$

1. Our classification algorithm has the features : it assigns a class to every point of an object $X$, whereas the classification was limited to a few types of points in previous work [MR80].

2. It should be pointed out that we propose a classification for every point of a object $X$, instead of a characterisation of only a few types of points as it was done in previous work [MR80].

3. For type A points, $C''$ is always equal to 1. Like in the 2D case, interior points may appear at the intersection of several surfaces (see figure 1).

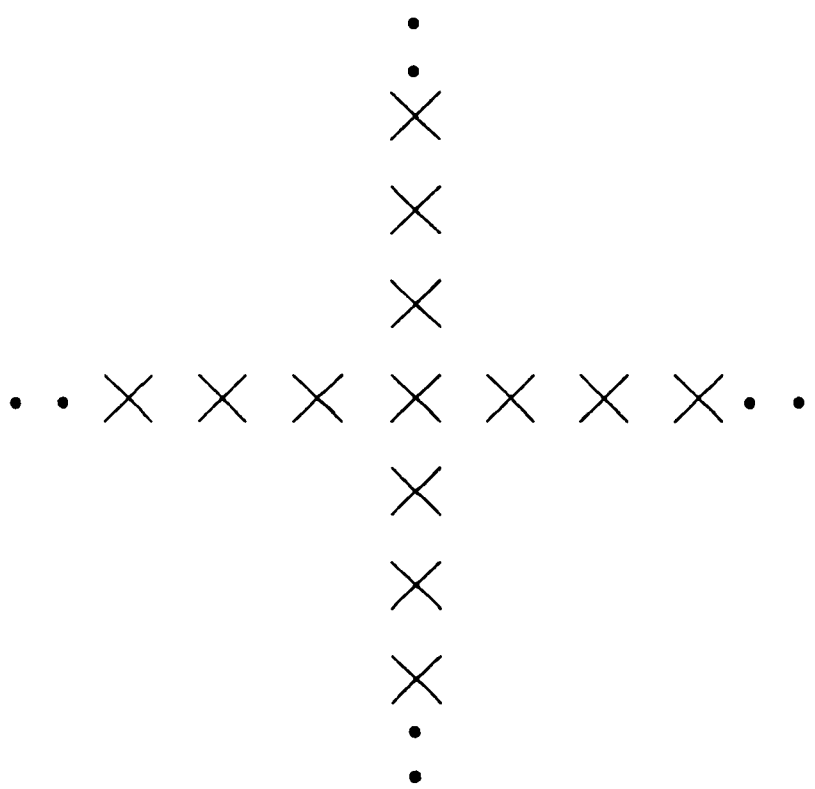

Figure 1: The horizontal trace of two intersecting vertical planes: the central point is an interior point.

4. Edge points may be of two types: simple points and non simple points. In fact it is clear that only edge points may be simple. The following property stands:

   a point $x \in X$ is simple iff:

$$x \text{ is an edge point} \tag{5}$$

$$NH[X \cap N_{26}(x)] = NH[X \cap N_{26}^{*}(x)] \tag{6}$$

$$NH[(\overline{X} \cap N_{26}^{*}(x)) \cup \{x\}] = NH[\overline{X} \cap N_{26}^{*}(x)] \tag{7}$$

In effect, conditions (6) and (7) are identical to conditions (3) and (4) of the original definition of simple points [Mor81].

Moreover, we have already seen that $NC'(X \cap N_{26}(x)) = C' = 1$, therefore condition (1) for simple points is equivalent to $C' = 1$.

Let $b$ represent the number of connected components in $\overline{X} \cap N_{26}^{*}(x)$ not adjacent to $x$. We have $NC'[\overline{X} \cap N_{26}^{*}(x)] = b + \overline{C}'$ and $NC'[(\overline{X} \cap N_{26}^{*}(x)) \cup \{x\}] = b + \overline{C}' = b + 1$. Hence the condition (2) for simple points is equivalent to $\overline{C}' = 1$. □

5. Simple surfaces may intersect without creating junction points. See for example figure 2 where two planes intersect : all points are classified as surface points. Connected components numbers are less powerful to describe junctions in discrete spaces than in continuous spaces. Nevertheless we present in section 5 a method to overcome this difficulty.

   The same problem still exists for junctions of curves. If we consider figure 2 as an intersection between several curves, we notice that all points are classified as curve points. We can overcome this difficulty by counting the neighbors of each curve points, if the number of neighbors is greater than 2, there is a junction between curves.

# 5 Topological segmentation into simple surfaces

As discussed above the connected components numbers do not allow, in a complex figure, to separate simple surfaces from each other (see figure 2) : if we delete all junction points of an image the remaining connected components are not necessarily simple surfaces.

Some work was done to characterize simple surfaces [MR80, Kim84, KF81]. Let us consider the definition of a simple surface proposed in [MR80] because a simple surface is considered here as a set of voxels rather than a set of faces like in [KF81]. We first compare this definition with our classification, then we show that this definition is not appropriate, finally we propose an algorithm for the complete extraction of simple surfaces.

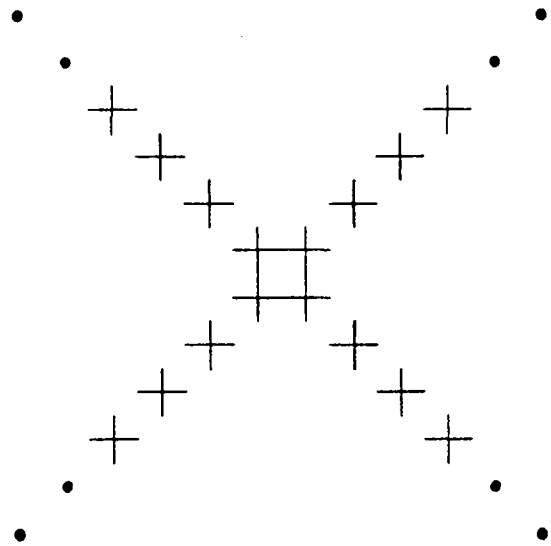

Figure 2: The horizontal trace of two intersecting vertical planes: all points are surface points.

A point $x \in X$ is a simple surface point, according to [MR80], if the following conditions are all satisfied :

1. $X \cap N_{26}^{*}(x)$ has exactly one component adjacent to $x$ (in the $X$ sense).
2. $\overline{X} \cap N_{26}^{*}(x)$ has exactly two components adjacent to $x$ (in the $\overline{X}$ sense); call these components $B_x$ and $C_x$.
3. for every $y \in X$ adjacent to $x$ (in the $X$ sense), $y$ is adjacent (in the $\overline{X}$ sense) to some point in $B_x$ and to some point in $C_x$.

If we use 26-connectedness for $X$, we can see that condition 1 is equivalent to $C^* = 1$, condition 2 is equivalent to $\overline{C} = 2$, hence these two conditions characterize what we call surface points. Let us consider now figure 2 : all points except the four central one's will be simple surface points. So this characterization succeeds in segmenting the complex surface into simple ones.

However we did not retain this definition because it is not always appropriate. In figure 3 one can see a set of points which should normally be interpreted as a simple surface: the central point of the $i$th plane is not a simple surface point according to the above definition.

To overcome this difficulty, we propose to use an approach based on an equivalence relation.

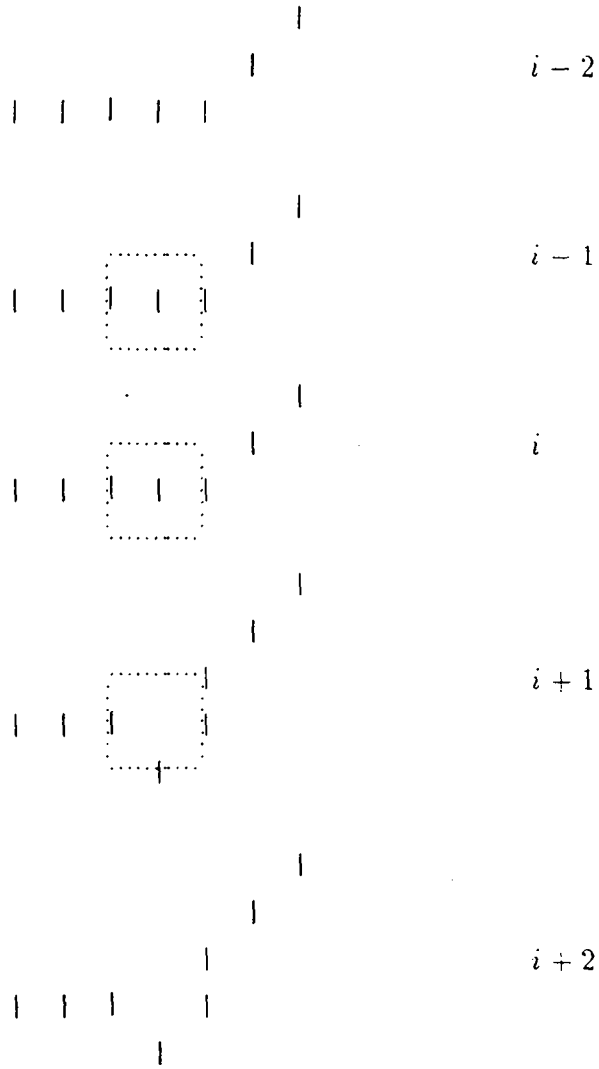


Figure 3: The point at the center of the window of the $i$th plane is not a simple surface point: the point at the upper right corner of the window in the $(i+1)$th plane does not satisfy condition 3.

Let $x$ be a surface point. We call $B_x$ and $C_x$ the two connected components of $\overline{X} \cap N_{26}^*(x)$ 6-adjacent to $x$. We say that two surface points $x$ and $y$ are in relation if there is a 26-path $x_0, x_1, \ldots x_i, \ldots x_n$ with $x_0 = x$ and $x_n = y$ such as for $i \in [0 \ldots n-1]$ :

- if $B_{x_i} \cap B_{x_{i+1}} \neq \emptyset$ and $C_{x_i} \cap C_{x_{i+1}} \neq \emptyset$
- or if $B_{x_i} \cap C_{x_{i+1}} \neq \emptyset$ and $C_{x_i} \cap B_{x_{i+1}} \neq \emptyset$.

It is easy to check that this relation is reflexive, symmetric and transitive, i.e. it is an equivalence relation.

We call simple surface any equivalence class of this equivalence relation. Let $x$ belong to a simple surface $S \subseteq X$. If $x$ has a 26-neighbor which does not belong to $S$ and which is not an edge point, we say that $x$ is a junction point of $S$.

We have now a topological segmentation of a 3D object into simple surfaces and surface junctions.

# 6 A new thinning algorithm

Several algorithms have been proposed for thinning 3D objects (see [Mor81, LVG80, TF82, TF81, HPJ84, GB90]. Two kinds of operations are considered : one kind reduces objects to surfaces and curves, the other one transforms them solely into curves. One basic idea is to remove in parallel simple points which satisfy some "geometrical" properties. Like in the 2D case, we have to use a cycle of several iterations in order to prevent some objects from vanishing (e.g. a two points thickness object). In the 3D case we can use a cycle of 6 iterations corresponding to the Up, Bottom, North, South, West, East directions.

We present now a new thinning algorithm whose the geometrical properties are based on connected components numbers.

**Algorithm** Do the following operations successively from the Up, Bottom, ... East sides of $X$ until there is no changes:

1. detect all surface points and all curve points. Label them as end points.
2. delete all edge points from a given side of $X$, provided they are simple and are not labeled.

It should be pointed out that once a point is labeled, it remains labeled in further iterations. If it was not the case a simple surface will be shrunk by its edge. In fact one

can see that the edge points of a simple surface will be deleted at the first cycle. All other points will be labeled at the first iteration so that no other points will be removed. Similarly a simple curve will have its end points removed. Other points will remain. It follows that the thinning algorithm preserves surfaces and curves except the very edge points and extremities. An example is shown in figure 4: a sharp corner generates a surface in the thinning process. Less sharp corners do not generate a surface. Hence this algorithm is well suited for describing objects which is composed of elongated parts. Other conditions may be used for end points in order to detect less sharp corners. This will not be discussed here.

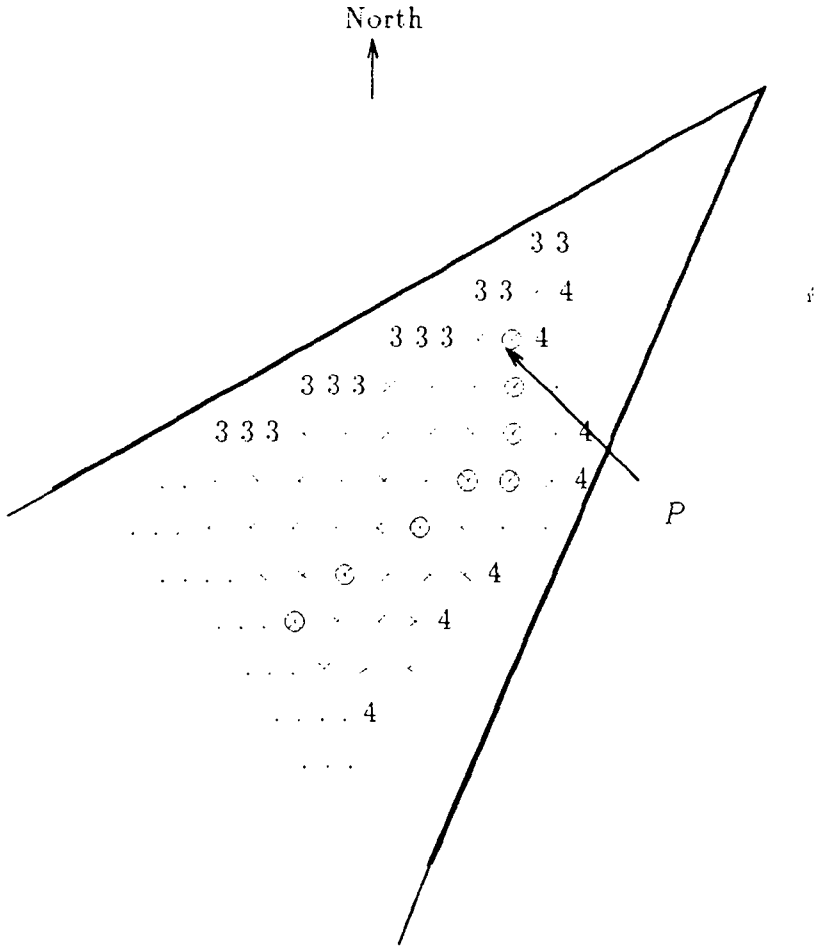


Figure 4: The horizontal trace of a "corner". All other planes are identical to this one. The point $P$ is detected at the 5th iteration as surface point and generates a branch encircled.

We have to mention that the proposed algorithm needs two steps at each iteration. All points must be treated by the first step before beginning the second one. In fact it is easy to modify the algorithm in order to have independent steps. This can be done by using other

labels. It allows to have an algorithm which can be implemented on a sequential computer more efficiently: each iteration can be done with a single scanning of the image.

# 7 Distance Transformation on simple surfaces

Distance transformation is a very important computation for many applications. It can be very useful for extracting dimensional characteristics of an object, or for estimating distance between several objects.

In previous work (see [Bor84] for example), distance transformations are proposed for binary pictures, consisting of feature and nonfeature elements. These transformations compute for each element an approximation of the distance to the nearest feature element.

We propose a new type of distance transformation for ternary pictures, consisting of feature elements, nonfeature elements and background elements. This new algorithm computes for each nonfeature element an approximation of the distance to the nearest feature element using a path consisting of nonfeatures elements.

## 7.1 Classical algorithm

We present algorithms computing a 3-D distance transformation algorithms whose can be easily extended to higher dimensions.

A classical algorithm consists of the successive application of two stages (forward and backward). Each stage consists in applying a specific mask (see figure 5) on a two-valued image : zero for feature elements and infinity otherwise (for nonfeature elements).

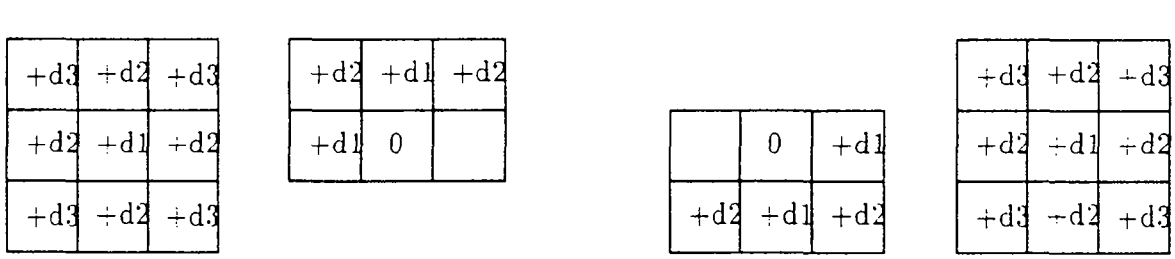


Figure 5: 3-D masks for the three-dimensional distance transformations

The forward mask is moved over the image from the left to the right, from the top to the bottom and from the front to the back. For each voxel, the sum of each 14-neighbors with the corresponding mask value is computed, and the new value of the voxel is the minimum of these sums. The backward mask is moved in the opposite way, and new values are computed identically.

Some values of $d1$, $d2$, and $d3$ :

- Using $d1 = 1$ and $d2 = d3 = \infty$ we obtain the 6-neighbor distance or city block distance.
- Using $d1 = d2 = d3 = 1$ we obtain the 26-neighbor distance or chessboard distance.

## 7.2 Distance on simple surfaces

Computing distances on simple surfaces will be helpful for understanding their geometry. It makes it easy to erode a surface or to compute its skeleton.

We compute the distance on the surface from the its border. Using our topological classification, we know that the border of a simple surface consists of edge and junction points. These special points will be feature elements, simple surface points will be nonfeature elements (the background remains unchanged).

We transform an image into a ternary image which is three-valued : zero for feature elements, infinity for nonfeature elements and a negative number for bakground elements.

Our algorithm consists of two stages which will be iterated until stabibility. We use the same masks as the ones used by the classical algorithm (see figure 5).

The forward mask is moved over the image from the left to the right, from the top to the bottom and from the front to the back. For each *nonfeature* voxel, the sum of each *nonfeature* or *feature* 14-neighbors with the corresponding mask value is computed, and the new value of the voxel is the minimum of these sums. The backward mask is moved in the opposite way, and new values are computed identically.

The speed of convergence depends on the shape of the simple surface.

# 8 Experimental Results

We considered two X-Ray scanner 3-D images of a vertebra scanned in two different positions (see figures 6 et 7). These images come from the Rennes Hospital in France, and are a courtesy of Pr. J.L. Coatrieux. They contain about 256x256x50 voxels (each voxel is $0.5 * 0.5 * 1\text{mm}^3$) whose intensity is coded with 256 discrete values.

In effect, both vertebras can be registered by the application of a geometric transformation which is the combination of a translation, rotation and three different scalings along three orthogonal principal axes. This transformation was computed by matching globally the sets of data points : the rotation angle is 30 degrees along an axis which is tilted of 11 degrees with respect to the vertical axis and scaling is close to 0.9 in two directions.

## 8.1 Thinning edge detection results

We applied a 3-D edge detector due to Monga, Deriche and Canny [MDMC90] to the original data to extract the external surface trace of the vertebras. A result is shown in figure 8, where the detected edge points are thresholded local maximum of the gradient magnitude in the direction of the gradient. We applied the described thinning algorithm to the result to obtain a simple surface, By doing this, we suppressed more than 20% of the number of edge points, still preserving the topology of surfaces. We show in figure 9 the result.

## 8.2 Distance on simple surfaces

We applied our distance transformation on simple surface to a 3-D cylinder in which we removed a point. We used the chamfer distance for the computation, it takes 28 seconds of CPU time on a DEC 5000. We show in figure 10 the result.

## 8.3 Topological classification and segmentation results

We applied the thinning algorithm to the entire 3-D object, producing a skeleton shown in figure 11. These skeletons each contain about 14,000 points, a figure which must be compared to the 170,000 original data points in each 3-D-image. These skeletons, despite their instability to noise, are good examples for our algorithm because of the complexity of the surfaces they are made of.

Then, we applied our classification and simple surface extraction algorithm to label each skeleton point. This computation takes 40 seconds of CPU time on a DEC 5000. We show in figures 12 and 13 the main topological structures extracted for the two vertebras.

We extracted from these structures the junction points of both vertebras, then we applied the geometric transformation found between them (see figures 14 and 15). It is easy to check in figure 16 the accurate superposition of the extracted structures between the two vertebras. This shows the astonishing stability of the segmentation : a single quasi-rigid transformation can superimpose most of the structures within a tolerance of $\pm$ 1 voxel.

Instead of junctions, one can use extracted simple surfaces. In order to obtain a robust segmentation of our surfaces, we perform an erosion of order 2 of the simple surfaces from their border toward their interior. We use for that computation a thresholding of the result of our distance transformation on simple surfaces. We apply our characterisation and simple surface extraction algorithm to the result of erosion. We show the results in figures 17 and 18.

After this step of erosion, we apply a conditional dilatation of order 2 of the remaining simple surfaces with respect to the original skeleton. This is an opening of simple surfaces.

We extract the simple surfaces of this result and we label them. The result of the step of labelling is shown in figures 19 and 20.

It is easy to check that we succeed in segmenting our complex surfaces to several simple surfaces which are stable (for more than 80% of them) from one object to the other. This will be used with profit in a forthcoming 3-D matching algorithm.

# 9 Conclusion

We have proposed a new approach to segment a discrete 3-D object into different classes of points which represent structures. The basic idea of this segmentation is the use of two local measures based on very local computations which allow massively parallel implementation. We obtain therefore a very fast segmentation of 3-D objects.

The proposed classification gives a very efficient set of structures, junctions or simple surfaces, which will allow more efficient registration of complex 3-D objects.

We applied our method to the segmentation into simple surfaces of the 3-D skeleton of a complex 3-D object, and the result appears to be remarkably accurate and stable with respect to quasi-rigid transformation, despite the relative instability of the skeleton itself.

Our method applies to the segmentation of 3-D edges, provided that the edge detector preserves the topology of junctions, which is not the case for known 3-D edges detector.

Our futur work includes a new 3-D edge detector, and the application of our segmenation method on 3-D edges, as well as its use to demonstrate robust matching of quasi rigid complex 3-D objects.

# References


[ABB+89] N. Ayache, J.D. Boissonnat, E. Brunet, L. Cohen, J.P. Chièze, B. Geiger, O. Monga, J.M. Rocchisani, and P. Sander. Building highly structured volume representations in 3d medical images. In *Computer Aided Radiology*, 1989. Berlin, West-Germany.

[ABC+90] N. Ayache, J.D. Boissonnat, L. Cohen, B. Geiger, J. Lévy Véhel, O. Monga, and P. Sander. Steps toward the automatic interpretation of 3d images. In *Workshop on 3D imaging in Medecine*, Travemunde, R.F.A., June 1990. NATO. Edited by Springer.

[Bor84] G. Borgefors. Distance transformations in arbitrary dimensions. *Computer Vision, Graphics and Image Processing*, 27:321–345, 1984.

[GB90] W.X. Gong and G. Bertrand. A simple parallel 3d thinning algorithm. To appear, 10th Int. Conf. on Pattern Recognition, June 17–21 1990. Atlantic City.

[HPJ84] K.J. Hafford and K. Preston Jr. Three dimensional skeletonization of elongated solids. *Computer Vision, Graphics and Image Processing*, 27:78–91, 1984.

[KF81] N. Keskes and O. Faugeras. Surface simple dans $z^3$. In *3ème Congrès Reconnaissance des Formes et d'Intelligence Artificielle*, pages 718–729. AFCET, September 1981.

[Kim84] C.E. Kim. Three-dimensional digital planes. *IEEE Transactions on PAMI, PAMI 6*, 5:639–645, September 1984.

[KR89] T.Y. Kong and A. Rosenfeld. Digital to topology: introduction and survey. *Computer Vision, Graphics and Image Processing*, 48:357–393, 1989.

[LVG80] S. Logbregt, P.W. Verbeck, and F.C. Groen. Three-dimensional skeletonization: principle and algorithm. *IEEE Transactions on PAMI, PAMI 2*. 1:75–77, January 1980.

[MDMC90] O. Monga, R. Deriche, G. Malandain, and J.P Cocquerez. Recursive filtering and edge closing : two primary tools for 3d edge detection. In *First European Conference on Computer Vision (ECCV), April 1990, Nice, France*, 1990. also Research Report INRIA 1103.

[Mor80] D.G. Morgenthaler. Three-dimensional digital topology: the genus. Tr-980. Computer Science Center, University of Maryland, College Park, MD 20742, U.S.A., November 1980.

[Mor81] D.G. Morgenthaler. Three-dimensional simple points: serial erosion, parallel thinning, and skeletonization. Tr–1005, Computer Science Center, University of Maryland, College Park, MD 20742, U.S.A., February 1981.

[MR80] D.G. Morgenthaler and A. Rosenfeld. Surfaces in three-dimensional digital images. Tr–940, Computer Science Center, University of Maryland, College Park, MD 20742, U.S.A., September 1980.

[NA85] A. Nakamura and K. Aizawa. On the recognition of properties of three-dimensional pictures. *IEEE Transactions on PAMI, PAMI 7*, 6:708–713, November 1985.

[PR71] C.M. Park and A. Rosenfeld. Connectivity and genus in three dimensions. Tr-156, Computer Science Center, University of Maryland, College Park, MD 20742, U.S.A., May 1971.

[Ros80] A. Rosenfeld. Three-dimensional digital topology. Tr-936, Computer Science Center, University of Maryland, College Park, MD 20742, U.S.A., September 1980.

[San89] P. Sander. Generic curvature features from 3-d images. *IEEE Transactions on Systems, Man, and Cybernetics*, November 1989. Special Issue on Computer Vision.

[TF81] Y.F. Tsao and K.S. Fu. A parallel thinning algorithm for 3d pictures. *Computer Vision, Graphics and Image Processing*, 17:315–331, 1981.

[TF82] Y.F. Tsao and K.S. Fu. A 3d parallel skeletonization thinning algorithm. *IEEE PRIP Conference*, pages 678–683, 1982.

[TYYF82] J.I. Toriwaki, S. Yokoi, T. Yonekusa, and T. Fukumura. Topological properties and topology-preserving transformation of a three-dimensional binary picture. In *Proceedings 6th Int. Conf. on Pattern Recognition*, pages 414–419, October 1982. Munich.

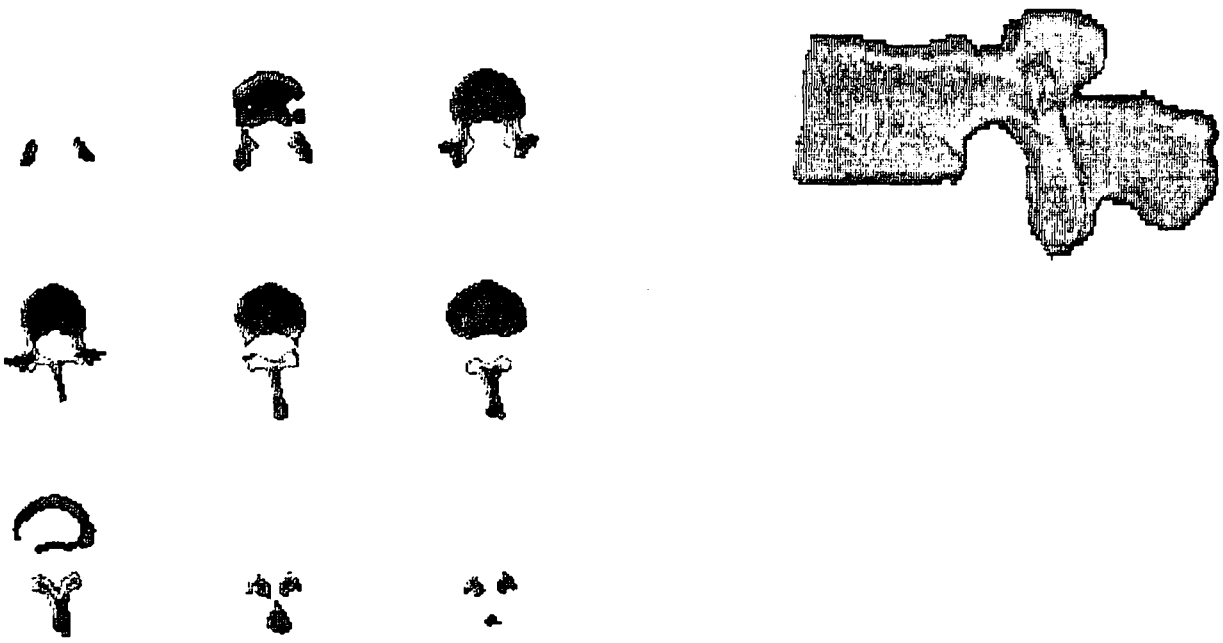

Figure 6: A few slices of the vertebra scanned in the first position and a 3-D representation (with rescaling in the third dimension) of this vertebra

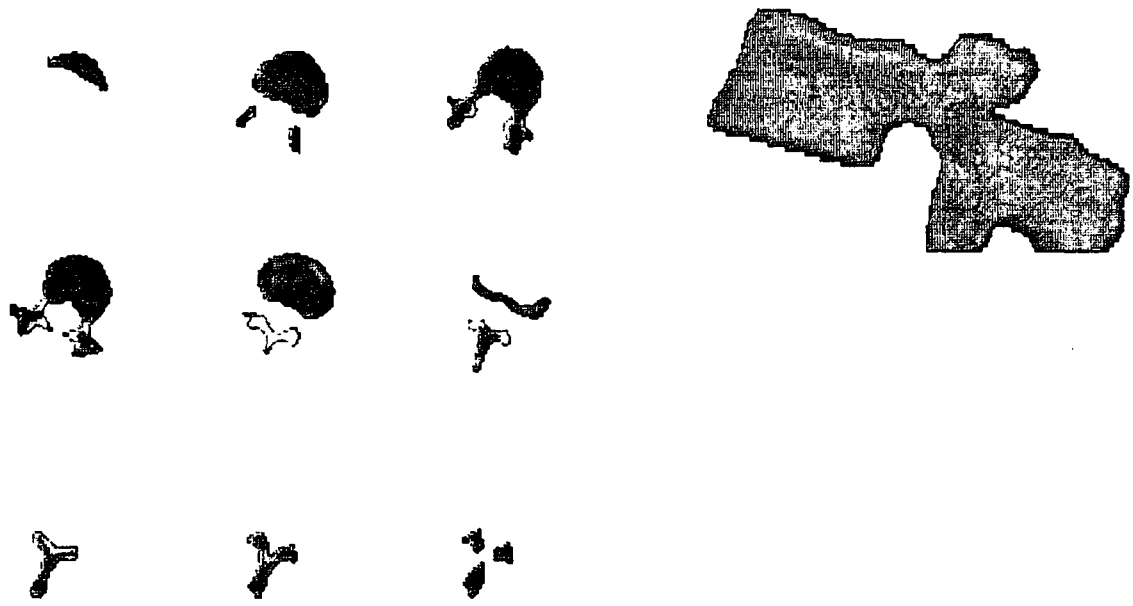

Figure 7: A few slices of the vertebra scanned in the second position and a 3-D representation (with rescaling in the third dimension) of this vertebra

Figure 8: A few slices of the detected edges of the vertebra in both positions

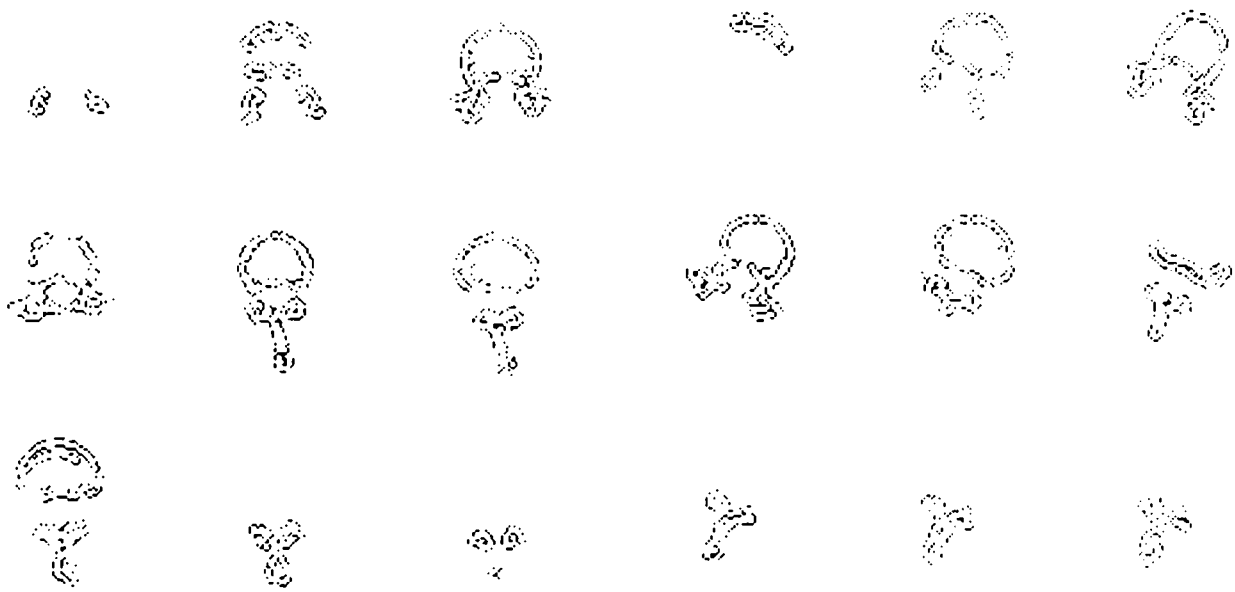

Figure 9: The edges points suppressed by the step of thinning in a few slices of the vertebra in both positions

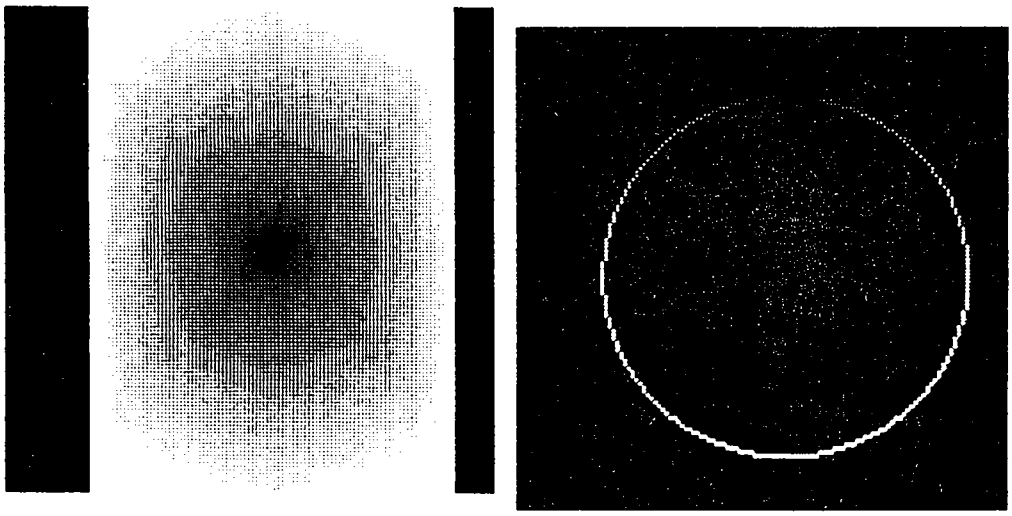

Figure 10: 3-D distance transformation on a cylinder. On the left (front view) the removed point is in front of the cylinder. On the right we show the slice with the removed point (at the top of the circle)

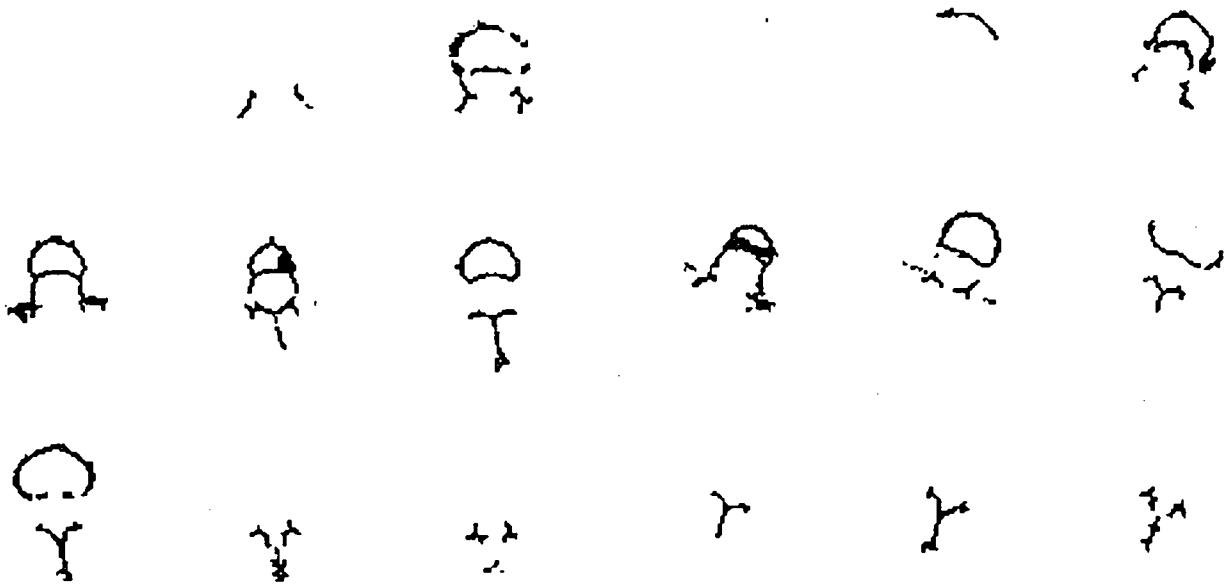

Figure 11: A few slices of the skeleton of the vertebra in both positions

Figure 12: Upper view of the skeleton of the vertebra in both positions. Surface points are dark grey, junction points are light grey and edge points are medium grey

Figure 13: 3-D representations of the skeleton of the vertebra in both positions (with rescaling in the third dimension). Surface points are dark grey, jonction points are light grey and edge points are medium grey

Figure 14: Projections on the XY-plane of the junction points of the skeleton of both images of the vertebra, and of the first vertebra after the computed transformation

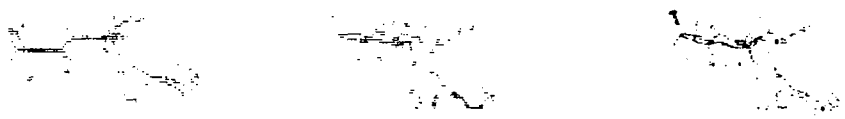

Figure 15: Projections on the YZ-plane of the junction points of the skeleton of both images of the vertebra, and of the first vertebra after the computed transformation

Figure 16: The result of the intersection of the dilated set of jonction points of the second vertebra's skeleton with the jonction points after transformation of the first vertebra skeleton in XY-plane and YZ-plane. All displayed points can be matched by the same quasi-rigid transformation with an accuracy of $\pm$ 1 voxel

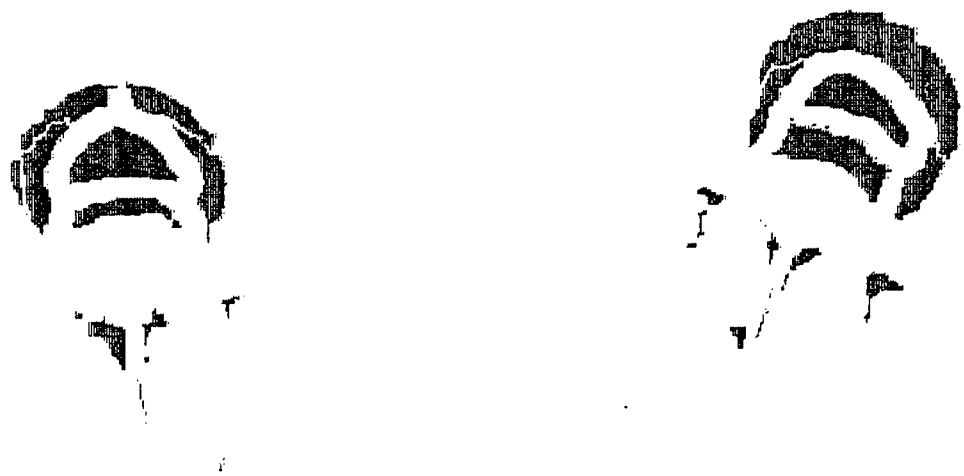

Figure 17: Upper view of the skeleton of the vertebra in both positions after an erosion of order 2

Figure 18: Front view of the skeleton of the vertebra in both positions after an erosion of order 2 (without rescaling in the third dimension)

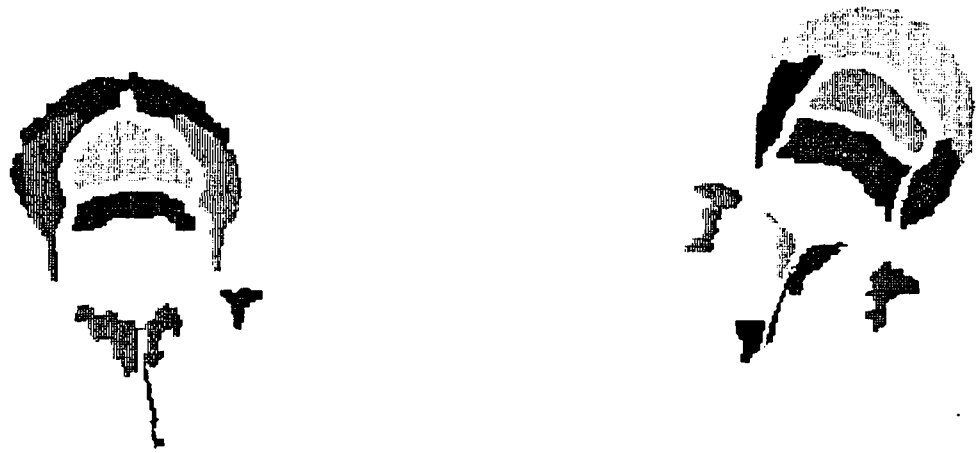

Figure 19: Upper view of the skeleton of the vertebra in both positions after the labelling of simple surfaces remaining after an opening of order 2

Figure 20: Front view of the skeleton of the vertebra in both positions after the labelling of simple surfaces remaining after an opening of order 2 (without rescaling in the third dimension)



Imprimé en France
par
l'Institut National de Recherche en Informatique et en Automatique.

ISSN 0249-6399